Clin Neuroradiol (2016) 26:341–346
DOI 10.1007/s00062-015-0370-6

ORIGINAL ARTICLE

Imaging Features of Pilocytic Astrocytoma in Cerebral Ventricles

JG. Xia · B. Yin · L. Liu · YP. Lu · DY. Geng · WZ. Tian

Received: 28 August 2014 / Accepted: 8 January 2015 / Published online: 28 January 2015

Abstract
Purpose Our aim was to identify imaging characteristics of pilocytic astrocytomas (PAs) in the cerebral ventricles to help radiologists distinguish PAs from other brain tumors preoperatively.
Methods Twelve postsurgery patients with a pathological PA diagnosis were included. Among them, 10 had submitted to surgery based on 3.0-T magnetic resonance imaging sequences and 7 because of computed tomography (CT) results. We analyzed their clinical and radiological records retrospectively.
Results The 12 patients (7 were male) had 13 lesions (11 with a single focus, 1 with multiple foci). Average age was 26.5 years (range, 6–49 years). Clinical symptoms included headache, dizziness, vomiting, and unstable gait. Tumor locations were the lateral ventricle (4), fourth ventricle (7), or both ventricles (1, but multifocal). One tumor had disseminated. PA diameters were 18.7–63.0 mm (mean ± standard deviation, 36.5 ± 12.4 mm). Nine had a round margin, and four had irregular margins. Two were cystic lesions. Eleven were mixed cystic and solid. CT showed the tumors as low-density masses. Two had calcifications. Their cystic portions showed low signal intensity (SI) on T1-weighted imaging (T1WI) and high SI on T2-weighted imaging (T2WI). The cystic walls and solid portions of the PAs showed slightly low SI on T1WI and slightly high SI on T2WI. After gadopentetate dimeglumine administration, the solid portion showed heterogeneous enhancement, whereas the cystic portion showed no enhancement.
Conclusions Radiological features of intraventricular and extraventricular PAs were similar to typical ones, including enhanced nodules within cysts. Radiological findings can usually diagnose PAs correctly.

Keywords Pilocytic astrocytoma · Computed tomography · X-ray · Computer · Magnetic resonance imaging

Introduction

The pilocytic astrocytoma (PA) is an unusual glioma in the central nervous system that is characterized by slow growth. According to the World Health Organization's 2007 classification of nervous system tumors, PAs are listed as grade I astrocytomas and account for 2.3 % of all primary central nervous system tumors in the patient population and 8.0–23.5 % of central nervous system tumors in the pediatric patient population [1–3]. PAs are usually benign astrocytomas that are circumscribed. They only rarely invade the surrounding brain tissues or lead to malignant manifestations, such as anaplasia, meningeal dissemination, or local recurrence.

JG. Xia, B. Yin, L. Liu, and YP. Lu contributed equally to this work and should be considered co-first authors.

WZ. Tian, MD (✉) · JG. Xia, MD
Department of Radiology, Jiangsu Taizhou People's Hospital,
230 YinChun Road,
225300 Taizhou, Jiangsu, China
e-mail: ybxjgtg@163.com

B. Yin, MD · YP. Lu, MD · DY. Geng
Department of Radiology, Huashan Hospital, Fudan University,
12 Wulumuqi Rd. Middle,
200040 Shanghai, China

L. Liu, MD
Department of Radiology, Shanghai Cancer Center, Fudan University,
270 Dongan Rd.,
200032 Shanghai, China

Most PAs are localized in or near the midline and mainly arise from the cerebellum, only secondarily emerging from the visual pathway, hypothalamic area, diencephalon, or brain stem [4, 5]. Because of their low ventricular incidence, only a few articles have described intraventricular PAs. This study was designed to analyze retrospectively the radiological images and clinical manifestations of 12 patients with intraventricular PAs after confirmation by operation and pathology in the Huashan Hospital. This summary of the radiological features of intraventricular PAs could increase the accuracy of their preoperative diagnosis.

Materials and Methods

Subjects

Between January 2008 and April 2014, we retrospectively reviewed the picture archive and communication system (PACS; GE Medical Systems, Milwaukee, WI, USA) and enrolled all patients who presented with a pathologically proven PA in their cerebral ventricles. Each subject had been submitted to surgery at the Huashan Hospital. A total of 12 patients (5 men, 7 women; mean age, 26.5 years; range, 6–49 years) with PAs confirmed by operation and pathology at the Huashan Hospital were recruited to our study.

Informed consent was obtained from all of the subjects. Our institutional review board approved the study.

Imaging Technique and Evaluation

Ten patients underwent magnetic resonance imaging (MRI) examinations. All MR images were acquired on a GE 3.0-T system (GE Medical Systems), which is equipped with an eight-channel head coil. MRI was performed using the following routine sequences: axial precontrast T1-weighted images, axial T2-weighted images, axial fluid-attenuated inversion recovery, and diffusion-weighted images (single-shot, spin-echo, echo-planar imaging sequences), with the following parameters: repetition time/echo time, 4800/minimum ms; b-values of 0 and 1000s/mm^2 in three orthogonal directions. Contrast-enhanced T1-weighted images were obtained in the axial and sagittal planes after intravenous contrast injection (gadopentetate dimeglumine, 0.1 mmol/kg).

Additionally, seven patients underwent computed tomography (CT) in the supine position with multiple spiral CT scans (Lightspeed; GE Medical Systems) with the following parameters: working voltage, 120 kV; current, 150–230 mA; slice thickness, 5 mm; matrix, 256 × 256.

Two experienced neuroradiologists retrospectively reviewed all of the CT and MRI images. The images were specifically evaluated for lesion size and shape, presence of calcification, attenuation and signal intensity, enhancement characteristics, peritumoral edema, and associated hydrocephalus. The neuroradiologists, who were blinded to the histological findings, calculated the mean apparent diffusion coefficient (ADC) values by means of a Functool software program (GE Medical Systems). To minimize variability, the regions of interest (ROIs) ranged between 0.5 and 3.0 cm^2 and differed according to the size and morphology of the tumors. They were placed manually in the solid part of the tumor. For ADC quantification, the ROIs were positioned in tumor parts that showed the lowest ADCs. The diffusion-weighted imaging (DWI) signal intensity of tumors was evaluated and was classified as hypointense, isointense, or hyperintense compared with that of the white matter. In addition, certain clinical data such as age, sex, symptoms, and duration of symptoms were reviewed.

All patients underwent surgical resection. Histological examinations were then performed in all 12 specimens.

Statistical Analysis

The statistical significance of the mean ADCs between the tumors and white matter was assessed by means of independent sample *t*-tests. $P < 0.05$ was considered to indicate statistical significance. All the analyses were performed using SPSS version 13.0 for Windows (SPSS Inc., Chicago, IL, USA).

Results

Baseline Patient and Clinical Data

Between January 2008 and April 2014, a total of 12 patients (5 men, 7 women; mean age, 26.5 years; range, 6–49 years) with PAs confirmed by intraoperative and pathological evaluations performed at the Huashan Hospital were recruited to our study. Their clinical, radiological, and histological features are summarized in Table 1. The course of the disease ranged from 3 weeks to 5 months. Symptoms included headache ($n = 9$), unstable gait ($n = 6$), dizziness ($n = 4$), vomiting ($n = 5$), and hypopsia ($n = 1$). One patient, with a PA in the lateral ventricle, accidently discovered the tumor after a traffic accident (he had noted no previous discomfort).

There were 13 lesions in 12 patients (11 had a single focus, 1 had multiple foci). Eight PAs were located in the fourth ventricle, two in the left lateral ventricle, and three in the right lateral ventricle. One had disseminated into the cerebrospinal fluid (CSF; Case 6). One patient exhibited evidence of PAs with multiple lesions, one in the lateral ventricle and one in the fourth ventricle. The latter grew along the lateral fossa of the fourth ventricle, invading the brain stem (Fig. 1).

Table 1 Neuroradiological manifestations of 12 intraventricular pilocytic astrocytomas

Case/gender/age (years)	Location/compositions	Morphology	Tumor size (mm)	CT attenuation	T1WI	T2WI	Enhancement	Hydrocephalus/peritumoral edema	Recurrence
1/M/37	Right LV/mixed cystic and solid	Oval	25 × 24 × 21	Low density	Hypointensity	Hyperintensity	Heterogeneous	+/−	–
2/M/49	Left LV/cystic	Oval	23 × 27 × 22	Low density	Hypointensity	Hyperintensity	No	+/−	–
3/F/30	Fourth ventricle/cystic	Oval	19 × 26 × 22	–	Hypointensity	Hyperintensity	Partial enhancement of cystic wall	+/+	–
4/M/8	Fourth ventricle/mixed cystic and solid	Irregular	50 × 42 × 43	Slightly low density	–	–	–	+/−	–
5/F/6	Fourth ventricle/mixed cystic and solid	Oval	2.7 × 2.5 × 2.2	Slightly low density	Hypointensity	Hyperintensity	Heterogeneous	+/−	Recurrence 4 years later
6/F/32	Fourth ventricle/mixed cystic and solid	Irregular	26 × 45 × 34	High density	Mixed signal intensity	Mixed signal intensity	Heterogeneous	+/−	–
7/M/29	Right LV, fourth ventricle/mixed cystic and solid	Oval irregular	32 × 40 × 30 25 × 30 × 32	–	Hypointensity	Heterogeneous hyperintensity	Heterogeneous	+/−	–
8/M/44	Left LV/mixed cystic and solid	Oval	17 × 12 × 18	Slightly low density	Hypointensity	Heterogeneous hyperintensity	Heterogeneous	—/−	–
9/F/16	Fourth ventricle/mixed cystic and solid	Oval	40 × 41 × 38	–	Hypointensity	Hyperintensity	Heterogeneous	+/−	Recurrence half a year later
10/F/10	Fourth ventricle/mixed cystic and solid	Irregular	63 × 38 × 50	–	Hypointensity	Heterogeneous hyperintensity	Heterogeneous	+/−	Recurrence 4 years later
11/F/44	Right LV/mixed cystic and solid	Oval	30 × 40 × 28	Slightly low density	–	–	–	+/−	–
12/F/13	Fourth ventricle/mixed cystic and solid	Oval	41 × 43 × 35	–	Hypointensity	Heterogeneous hyperintensity	Heterogeneous enhancement with cystic wall enhanced	+/+	–

CT computed tomography, *M* male, *F* female, *T1WI* T1-weighted imaging, *T2WI* T2-weighted imaging, *LV* lateral ventricle

The radiological findings for the PAs included well-defined margins. Nine had an oval shape, and four were irregularly shaped. The average diameter of these PAs were 36.5 ± 12.4 mm (range, 18.7–63.0 mm). Among the 13 PAs, we identified peritumoral edema in 2. Concerning the tumor compositions, 11 were mixed cystic and solid, with the solid region representing most of the tumor (Fig. 2), and two were completely cystic (Fig. 3). None of the patients showed any obvious hemorrhaging. All tumors had relatively well-circumscribed margins. Their cystic portions were strongly T2 hyperintense/T1 hypointense, closer to that of CSF. On DWI, they had low/iso signal intensity without enhancement. Solid portions were moderately T2 hyperintense/T1 hypointense with heterogeneous enhancement. In two cases, the cyst wall was enhanced. CT findings corresponded with the more profound hypointensity of cystic portions and less

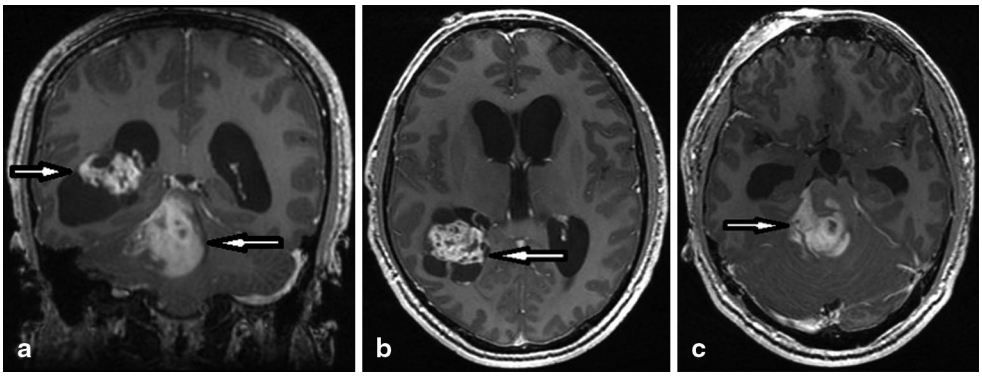

Fig. 1 Multiple pilocytic astrocytomas (PAs). **a** Coronal enhanced T1-weighted magnetic resonance (MR) images show the lesions located in the posterior crus of the right lateral ventricle and the fourth ventricular area (*arrow*). **b** Axial enhanced T1-weighted MR images indicate a mixed cystic and solid lesion on the posterior crus of the right ventricle (*arrow*). The solid portion was obviously enhanced, in contrast with the unenhanced cystic region. Additionally, the supratentorial cerebral ventricle was enlarged. **c** Axial-enhanced T1-weighted MR images show the lesion in the fourth ventricle, which mainly comprised an obviously enhanced solid portion. This PA grew along the lateral fossa of the fourth ventricle and invaded the brain stem (*arrow*)

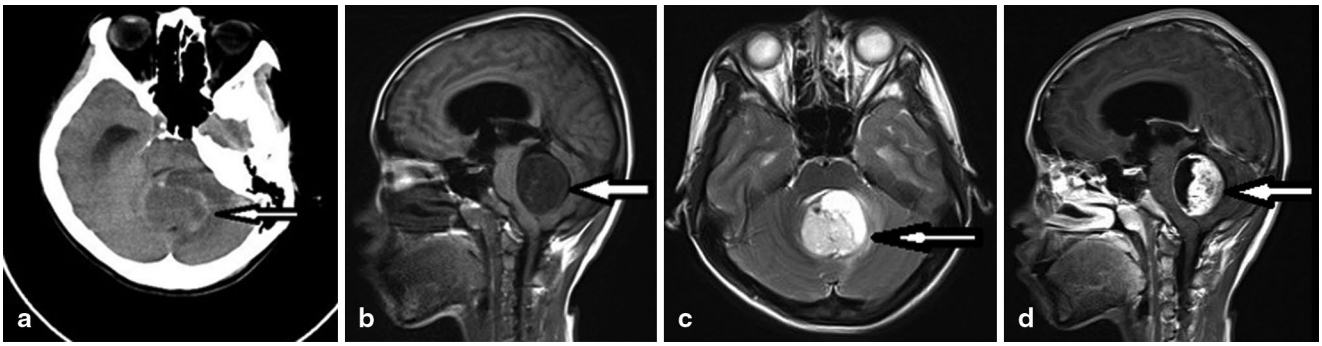

Fig. 2 Mixed cystic and solid pilocytic astrocytoma in the fourth ventricle. **a** Computed tomography scans suggest an oval low-density lesion in the fourth ventricle that was surrounded by calcification (*arrow*). **b** Sagittal T1-weighted magnetic resonance (MR) images show the lesion at low signal intensity with clear margins (*arrow*) and an enlarged supratentorial brain ventricle. **c** Axial T2-weighted MR images suggest that the solid region gave off high signal intensity, whereas the cystic region produced a fluid signal (*arrow*). **d** Sagittal-enhanced T1-weighted MR images show that not only the solid part but also the cystic wall of the lesion is obviously enhanced(*arrow*). The cystic region, however, has no such enhancement

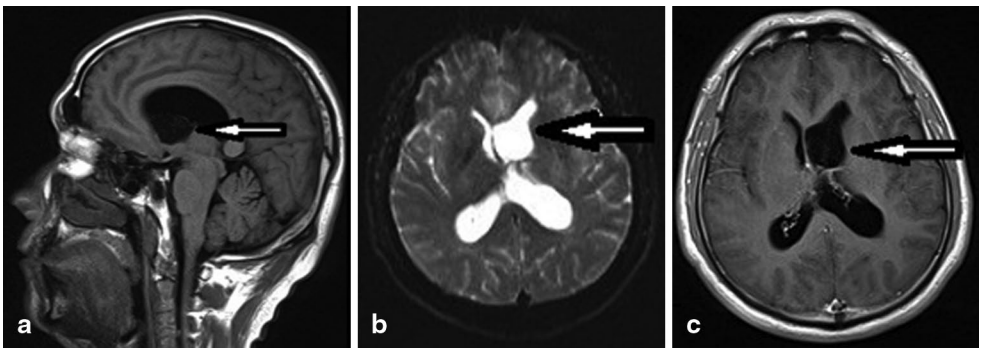

Fig. 3 Cystic pilocytic astrocytoma in the lateral ventricle. **a** Sagittal T1-weighted magnetic resonance (MR) images show the cystic lesion at low signal intensity with clear margins (*arrow*) and an enlarged supratentorial brain ventricle. **b** Axial T2-weighted MR images show the lesion located in the anterior crus of the left lateral ventricle with a fluid signal (*arrow*). **c** Sagittal-enhanced T1-weighted MR images suggest no enhancement of the lesion (*arrow*)

profound hypodensity of solid portions. Calcifications were present in two patients (Fig. 2).

On DWI, the signal intensity of the solid parts of the tumors was variable in 11 patients, with 2 being hyperin-

tense and 9 isointense. The mean lowest ADC values for the tumors and white matter were $1.46 \pm 0.50 \times 10^{-3}$ and $0.71 \pm 0.14 \times 10^{-3}$ mm^2/s, respectively. There was a statistically significant difference between the ADC values for the tumors and the white matter ($P = 0.03$, i.e., < 0.05).

Discussion

The PA is a distinctive histologic subtype of astrocytoma that occurs predominantly in children and adolescents. PA in the ventricle is relatively rare, accounting for approximately 4–15.6% of all PAs [6, 7]. The ventricular system comprises ependymal and choroid plexus tissues and lacks any astrocytic composition, Therefore, all intraventricular astrocytomas are derived from brain tissue around, and growing into, the ventricles. Based on their radiological features, we define astrocytomas derived from these structures around the ventricles—which in fact are mainly located in the ventricles—as intraventricular astrocytomas [8]. PAs are usually seen in children and adolescents younger than 20 years, and the incidence decreases with age [9]. They are seldom seen in people older than 30 years and are even rarer in those older than 50 years [10]. In our study, the ages of the 12 patients ranged from approximately 6 to 49 years, including 4 patients older than 30 years and none older than 50 years. There was no sex difference in the incidence of PAs in the present study, in accordance with previous reports. Our results showed a male/female ratio of a 5:7, which also corresponds to values in the literature [5, 10].

Some studies have reported a special relation between location and age [1, 11, 12]. One such study with a large sample, reported by Burkhand et al. [11], found that subtentorial cerebellar PAs always occurred in children but that supratentorial PAs occurred more often in adults. No age difference was found for PAs of the brain stem. In our study, most PAs in the fourth ventricle were seen in children, whereas PAs in the lateral ventricles occurred in adults—again in accordance with reports in the literature.

The clinical symptoms of PA are related to the size of the tumor, its location, and the existence of hydrocephalus. The course of PA is always over a period of several months [10]. Patients with PAs have clinical symptoms, including headache, vomiting, mental disorders, ataxia, and dystopia, among others [12]. In our study group, the course of the disease ranged from 3 weeks to 5 months, with headache ($n = 9$), unstable gait ($n = 6$), dizziness ($n = 4$), vomiting ($n = 5$), and hypopsia ($n = 1$). One patient with PA in the lateral ventricle accidently discovered the tumor after a traffic accident. There had been no prior discomfort. Except for one case of PA in the triangular area of the left lateral ventricle, all patients had hydrocephalus of different degrees, especially those with PAs in the fourth ventricle.

The radiological manifestations of intraventricular PA are similar to those of other PAs of the brain. In our cases, all of the lesions had clear margins. Most of them were mixed cystic and solid ($n = 11$), except for the small portion of lesions that were totally cystic. PA typically manifests as a cystic lesion with mural nodules that are enhanced after injection of contrast agents.

Histologically, PA is characterized by elongated, thin, highly spindled tumor cells. PA classically manifests in a noteworthy biphasic pattern comprising a combination of loose glial tissue and compact piloidal tissue. The piloidal tissue components include dense sheets of elongated bipolar cells that demonstrate the highly distinctive feature of fine fibrillary (hair-like) processes and a typical abundance of Rosenthal fibers. In contrast, the loose glial tissue is composed of multipolar cells, microcapsules, and eosinophilic granular bodies. The various components of compact and loose tissues generate the differing proportions of solid and cystic regions in the tumor. Some tumors have a predominance of the glial component, whereas the preponderance of piloidal tissue in other tumors illustrates the varying radiological manifestations of PAs. Among the 13 lesions in our study, 2 were cystic, and 11 were mixed cystic and solid. The solid nodules in the mixed cystic and solid PAs were obviously heterogeneously enhanced. There are abundant vessels in PAs that have a large gap in the capillary basement membrane, sometimes in addition to glomeruloid vascular structures. These capillaries are fenestrated and increase vascular permeability, which would facilitate the entrance of more contrast agent into the tumor tissue via the epithelial gap of the vessels but not via the blood–brain barrier [5, 13]. The cystic wall of the tumor is selectively enhanced. In our group, the cystic walls of two lesions became enhanced. Unenhanced cystic walls always comprise the reactive hyperplasia of glial or compressed brain tissues that cannot be resected during an operation. The pathological basis of this enhancement of the cystic wall remains controversial, as most researchers correlate this phenomenon with active tumor cells and neovascularization in the cystic wall. A study by Beni-Adani et al. [14], however, found no tumor cells on the enhanced cystic walls, and no recurrence was observed 4 years after resection. Thus, they suggested that this enhancement was due to reactive hyperplastic vessels.

Most of the solid parts of the tumors were isointense on DWI. The mean ADC value of tumors was higher than the mean ADC value of white matter. The results of a previous study were similar to those in our study [15].

Hemorrhage, calcification, and CSF dissemination are seldom seen with PAs. In this study, we identified two cases of calcification. According to previous reports, approximately 4% of PAs are accompanied by CSF dissemination, potentially due to the tumor's destruction of the ependyma or the accumulation of tumor cells in the lacuna of the pia

mater via the intravascular or perivascular space, finally leading to dissemination or invasion into adjacent brain tissues [16, 17].

In summary, although intraventricular PA is rare, we should consider this diagnosis on finding a solid cystic mass with clear margins in the ventricular system. Compared with PAs in brain parenchyma, intraventricular PAs show classic manifestations. For example, a cyst with mural nodules was present, and the nodules were enhanced after contrast administration. Physicians can make a sound differential diagnosis of these tumors based on radiological findings combined with the patient's age.

Conclusions

This study revealed that the radiological features of intra- and extraventricular PAs are similar and that the nodules in PAs enhance similar to typical PAs. The radiological findings can usually provide a correct diagnosis.

Conflict of Interest None.

References

1. Stüer C, Vilz B, Majores M, Becker A, Schramm J, Simon M. Frequent recurrence and progression in pilocytic astrocytoma in adults. Cancer. 2007;110:2799–808.
2. Rickert CH, Paulus W. Epidemiology of central nervous system tumors in childhood and adolescence based on the new WHO classification. Childs Nerv Syst. 2001;17:503–11.
3. Rosemberg S, Fujiwara D. Epidemiology of pediatric tumors of the nervous system according to the WHO 2000 classification: a report of 1,195 cases from a single institution. Childs Nerv Syst. 2005;21:940–4.
4. Bilginer B, Nafin F, Oguz KK, Uzun S, Soylemezoglu F, Akalan N. Benign cerebellar pilocytic astrocytomas in children. Turk Neurosurg. 2011;21:22–6.
5. Koeller KK, Rushing EJ. From the archives of the AFIP: pilocytic astrocytoma: radiologic-pathologic correlation. Radiographics. 2004;24:1693–708.
6. Kumar AJ, Leeds NE, Kumar VA, Fuller GN, Lang FF, Milas Z, Weinberg JS, Ater JL, Sawaya R. Magnetic resonance imaging features of pilocytic astrocytoma of the brain mimicking high-grade gliomas. J Comput Assist Tomogr. 2010;34:601–11.
7. Cyrine S, Sonia Z, Mounir T, Badderedine S, Kalthoum T, Hedi K, Moncef M. Pilocytic astrocytoma: a retrospective study of 32 cases. Clin Neurol Neurosurg. 2013;115:1220–5.
8. Abel TJ, Chowdhary A, Thapa M, Rutledge JC, Geyer JR, Ojemann J, Avellino AM. Spinal cord pilocytic astrocytoma with leptomeningeal dissemination to the brain—case and review of the literature. J Neurosurg. 2006;105:508–14.
9. Malik A, Deb P, Sharma MC, Sarkar C. Neuropathological spectrum of pilocytic astrocytoma—an Indian series of 120 cases. Pathol Oncol Res. 2006;12:164–71.
10. Murray RD, Penar PL, Filippi CG, Tarasiewicz I. Radiographically distinct variant of pilocytic astrocytoma: a case series. J Comput Assist Tomogr. 2011;35:495–7.
11. Burkhard C, Di Patre PL, Schüler D, Schuler G, Yasargil MG, Yonekawa Y, Lütolf UM, Kleihues P, Ohgaki H. A population-based study of the incidence and survival rates in patients with pilocytic astrocytoma. J Neurosurg. 2003;98:1170–4.
12. Kim MS, Kim SW, Chang CH, Kim OL. Cerebellar pilocytic astrocytomas with spontaneous intratumoral hemorrhage in adult. J Korean Neurosurg Soc. 2011;49:363–6.
13. Grand SD, Kremer S, Tropres IM, Hoffmann DM, Chabardes SJ, Lefournier V, Berger FR, Pasteris C, Krainik A, Pasquier BM, Peoch M, Le Bas JF. Perfusion—sensitive MRI of pilocytic astrocytomas: initial results. Neuroradiology. 2007;49:545–50.
14. Beni-Adani L, Gomori M, Spektor S, Constantini S. Cyst wall enhancement in pilocytic astrocytoma: neoplastic or reactive phenomena. Pediatr Neurosurg. 2000;32:234–9.
15. Horger M, Vogel MN, Beschorner R, Ernemann U, Worner J, Fenchel M, Ebner F, Nagele T, Heckl S. T2 and DWI in pilocytic and pilomyxoid astrocytoma with pathologic correlation. Can J Neurol Sci. 2012;39:491–8.
16. Andreia VF, Geovani CAA, Veronica AZ, Ghizoni E, Queiroz LS. Dissemination patterns of pilocytic astrocytoma. Clin Neurol Neurosurg. 2006;108:568–72.
17. Figueiredo EG, Matushita H, Machado AG, Plese JPP, Rosemberg S, Marino R. Leptomeningeal dissemination of pilocytic astrocytoma at diagnosis in childhood: two cases report. Arq Neuropsiquiatr. 2003;61:842–7.